A Kinematic Analysis and Evaluation of Planar Robots Designed From Optimally Fault-Tolerant Jacobians

Khaled M. Ben-Gharbia, *Student Member, IEEE*,
Anthony A. Maciejewski, *Fellow, IEEE*,
and Rodney G. Roberts, *Senior Member, IEEE*

***Abstract*—It is common practice to design a robot's kinematics from the desired properties that are locally specified by a manipulator Jacobian. In this work, the desired property is fault tolerance, defined as the post-failure Jacobian possessing the largest possible minimum singular value over all possible locked-joint failures. A mathematical analysis based on the Gram matrix that describes the number of possible planar robot designs for optimally fault-tolerant Jacobians is presented. It is shown that rearranging the columns of the Jacobian or multiplying one or more of the columns of the Jacobian by ± 1 will not affect local fault tolerance; however, this will typically result in a very different manipulator. Two examples, one that is optimal to a single joint failure and the second that is optimal to two joint failures, are analyzed. This analysis shows that there is a large variability in the global kinematic properties of these designs, despite being generated from the same Jacobian. It is especially surprising that major differences in global behavior occurs for manipulators that are identical in the working area.**

***Index Terms*—Fault-tolerant robots, robot kinematics, redundant robots.**

I. Introduction

The design and operation of fault-tolerant manipulators is critical for applications in remote and/or hazardous environments where routine maintenance and repair are not possible. The failure rates for components in such harsh environments are relatively high [1]–[3].[1] Example applications include space exploration [5], [6], underwater exploration [7], and nuclear waste remediation [8], [9], where there has been a great deal of research to improve manipulator reliability [3], [10], design fault-tolerant robots [11], [12], and determine mechanisms for analyzing [13], detecting [14], [15], identifying [16]–[18], and recovering [19]–[22] from failures. Many of these component failures will result in a robot's joint becoming immobilized, i.e., a locked joint failure mode [14], [23]. In addition, component failures that result in other common failure modes, e.g., free-swinging joint failures [24], [25], are frequently transformed into the locked joint failure mode by failure recovery mechanisms that employ fail safe brakes [26].

A large body of work on fault-tolerant manipulators has focused on the properties of kinematically redundant robots, both in serial or parallel form [27]–[31]. These analyses have been performed both on the local properties associated with the manipulator Jacobian [32]–[35] as well as the global characteristics such as the resulting workspace following a particular failure [36]–[39]. (Clearly both local and global kinematic properties are related, e.g., workspace boundaries correspond to singularities in the Jacobian.) In this work it is assumed that one is given a set of local performance constraints that require a manipulator to function in a configuration that is optimal under normal operation and after an arbitrary single joint fails and is locked in position. Specifically, the desired Jacobian matrix must be isotropic, i.e., it should possess all equal singular values prior to a failure, and have equal minimum singular values for every possible single column being removed. Because these constraints do not result in a unique manipulator, one can then use global characteristics to distinguish between multiple manipulators that meet the local design criteria.

In this work, we focus on the characteristics of planar manipulator designs. This does not necessarily mean that the physical robot must operate in only two dimensions. For example, many robot designs can be decomposed into a planar portion along with an orthogonal portion, e.g., SCARA robots. Thus one approach to obtaining a higher reliability robot with a simpler design is to only apply the fault-tolerant techniques discussed here to the planar component.

The remainder of this paper is organized in the following manner. A local definition of failure tolerance centered on desirable properties of the manipulator Jacobian is mathematically defined in the next section. In Section III, the Gram matrix is used to describe all Jacobians with the same optimal fault tolerance properties. These results are used to present illustrative examples of manipulator designs that are generated from optimally fault-tolerant Jacobians in Section IV. The global properties of manipulators that possess the same Jacobian are analyzed and compared in Section V. An example is shown of an optimally fault-tolerant eight degree-of-freedom manipulator operating in a fully six-dimensional task space is shown in Section VI. The conclusions of this work are then presented in Section VII.

II. Background on Optimally Fault-Tolerant Jacobians

As was done in [40], the dexterity of a manipulator is quantified in terms of the properties of the manipulator Jacobian matrix that relates end-effector velocities to joint angle velocities. The Jacobian will be denoted by the $m \times n$ matrix J, where m is the dimension of the task space and n is the number of degrees-of-freedom of the manipulator. For redundant manipulators $n > m$, and the quantity $n - m$ is the degree of redundancy. The manipulator Jacobian can be written as a collection of columns

$$J_{m\times n} = [j_1 \quad j_2 \quad \cdots \quad j_n] \tag{1}$$

where j_i represents the end-effector velocity due to the velocity of joint i. For an arbitrary single joint failure at joint f, assuming that the failed joint can be locked, the resulting m by $n-1$ Jacobian will be missing the fth column, where f can range from 1 to n. This Jacobian will be denoted by a preceding superscript so that in general

$${}^{f}J_{m\times(n-1)} = [j_1 \quad j_2 \quad \cdots \quad j_{f-1} \quad j_{f+1} \quad \cdots \quad j_n]. \tag{2}$$

The properties of a manipulator Jacobian are frequently quantified in terms of the singular values, denoted σ_i, which are typically ordered so that $\sigma_1 \geq \sigma_2 \geq \cdots \geq \sigma_m \geq 0$. Most local dexterity measures can be defined in terms of simple combinations of these singular values such as their product (determinant) [41], sum (trace), or ratio (condition number) [42]–[44]. The most significant of the singular values is σ_m, the minimum singular value, because it is by definition the measure of proximity to a singularity and tends to dominate the behavior of both the manipulability (determinant) and the condition number. The

Manuscript received July 7, 2013; accepted November 4, 2013. Date of publication January 27, 2014; date of current version April 1, 2014. This paper was recommended for publication by Associate Editor J. Peters and Editor C. Torras upon evaluation of the reviewers' comments. This work was supported in part by the National Science Foundation under Contract IIS-0812437.

K. M. Ben-Gharbia and A. A. Maciejewski are with the Department of Electrical and Computer Engineering, Colorado State University, Fort Collins, CO 80523-1373, USA (e-mail: khaled.ben-gharbia@colostate.edu; aam@colostate.edu).

R. G. Roberts is with the Department of Electrical and Computer Engineering, Florida A&M–Florida State University, Tallahassee, FL 32310-6046, USA (e-mail: rroberts@eng.fsu.edu).

Color versions of one or more of the figures in this paper are available online at http://ieeexplore.ieee.org.

Digital Object Identifier 10.1109/TRO.2013.2291615

[1]One recent example is the Fukushima nuclear reactor accident, where robot component failures were not only likely, but inevitable [4].

minimum singular value is also a measure of the worst-case dexterity over all possible end-effector motions.

The definition of failure tolerance used in this work is based on the worst-case dexterity following an arbitrary locked joint failure. Because ${}^f\sigma_m$ denotes the minimum singular value of ${}^f J$, ${}^f\sigma_m$ is a measure of the worst-case dexterity if joint f fails. If all joints are equally likely to fail, then a measure of the worst-case failure tolerance is given by

$$\mathcal{K} = \min_{f=1}^{n}({}^f\sigma_m). \tag{3}$$

Physically, this corresponds to minimizing the worst-case increase in joint velocity when a joint is locked and the others must accelerate to maintain the desired end effector trajectory. In addition, maximizing $\mathcal{K}$ is equivalent to locally maximizing the distance to the postfailure workspace boundaries [1]. To insure that manipulator performance is optimal prior to a failure, an optimally failure tolerant Jacobian is further defined as having all equal singular values because of the desirable properties of isotropic manipulator configurations [42]–[44]. Under these conditions, to guarantee that the minimum ${}^f\sigma_m$ is as large as possible, they should all be equal. It is easy to show [33] that the worst-case dexterity of an isotropic manipulator that experiences a single joint failure is governed by the inequality

$$\min_{f=1}^{n}({}^f\sigma_m) \leq \sigma\sqrt{\frac{n-m}{n}} \tag{4}$$

where σ denotes the norm of the original Jacobian. The best case of equality occurs if the manipulator is in an optimally failure tolerant configuration. The above inequality makes sense from a physical point of view because it represents the ratio of the degree of redundancy to the original number of degrees of freedom.

Using the above definition of an optimally failure tolerant configuration, one can identify the structure of the Jacobian required to obtain this property [45].[2] In particular, one can show that the optimally failure tolerant criteria requires that each joint contributes equally to the null space of the Jacobian transformation [34]. Physically, this means that the redundancy of the robot is uniformly distributed among all the joints so that a failure at any joint can be compensated for by the remaining joints. Therefore, in this work, an optimally failure tolerant Jacobian is defined as being isotropic, i.e., $\sigma_i = \sigma$ for all i, and having a maximum worst-case dexterity following a failure, i.e., one for which ${}^f\sigma_m = \sigma\sqrt{\frac{n-m}{n}}$ for all f. The second condition is equivalent to having the columns of the Jacobian have equal norms.

The simplest example of an optimally failure tolerant configuration is given by the following Jacobian for a three degree-of-freedom planar manipulator:

$$J = [j_1 \quad j_2 \quad j_3] = \begin{bmatrix} -\sqrt{\frac{2}{3}} & \sqrt{\frac{1}{6}} & \sqrt{\frac{1}{6}} \\ 0 & -\sqrt{\frac{1}{2}} & \sqrt{\frac{1}{2}} \end{bmatrix}. \tag{5}$$

The null space at this configuration is given by $\sqrt{1/3}\,[1\ 1\ 1]^T$, which illustrates that each joint contributes equally to the null space motion, thus distributing the redundancy proportionally to all degrees of freedom. Geometrically, it is easy to see that the three vectors j_1, j_2, and j_3 are all 120° apart, which results in a balanced coverage of the planar workspace. If the three possible joint failures are considered, one can show that

$${}^f\sigma_2 = \sqrt{\frac{1}{3}} \tag{6}$$

for $f = 1$ to 3, which satisfies the optimally failure tolerant criterion. Given this example of an optimally failure tolerant J, one might be interested in designing the kinematics for a manipulator that would possess these qualities. In the next section, the Gram matrix is used to analyze the different number of manipulator kinematics that can result from a given fault-tolerant Jacobian.

III. Fault Tolerance and the Gram Matrix

As first shown in [40], the Gram matrix

$$G = J^T J \tag{7}$$

provides insight into the geometry and fault tolerance of a manipulator design. Here, the Jacobian J can be the positional, orientational, or the manipulator Jacobian. Some care concerning units should be exercised in the case of the manipulator Jacobian or when there is a mixture of revolute and prismatic joints. When a Jacobian is isotropic, the Gram matrix takes on a particularly simple form: If the singular values of J are equal to 1, then $G = J^T J = I - NN^T$, where the $n \times (n-m)$ matrix N consists of $(n-m)$ orthonormal null vectors of J. In the case of a manipulator with a single degree of redundancy, $G = I - \hat{\mathbf{n}}_J \hat{\mathbf{n}}_J^T$, where $\hat{\mathbf{n}}_J$ is the unit length null vector when J is in a non-singular configuration. The requirement for optimal fault tolerance specifies further conditions on the null space matrix N. Specifically, the rows of N must all have the same norm $\sqrt{\frac{n-m}{n}}$ and be spread out in a sense that will be made precise later.

Once an optimal Gram matrix is determined, an obvious and important question is to characterize all the corresponding Jacobians and Denavit and Hartenberg (DH) parameters for the corresponding manipulators. Clearly, a simple change in the base frame orientation through rotation and/or reflection will not change the basic robot structure. The difference in this case is simply a pre-multiplication of the Jacobian by an orthogonal matrix. For the sake of discussion, we will say that two configurations are *equivalent* if their corresponding Jacobians differ only by a pre-multiplication by an orthogonal matrix Q. For any n degree-of-freedom revolute jointed planar manipulator, denoted by n-R, it can be shown that two full rank Jacobians J and J' are equivalent if and only if $(J')^T J' = J^T J$, i.e., if their Gram matrices are equal.

Two planar n-R manipulators with equivalent Jacobians have essentially the same DH parameters, so the corresponding robot configurations can be considered to be the same in that sense. This is because when there is a change in the orientation of the base frame, either through a rotation or a combination of a rotation and reflection, the new Jacobian merely differs from the original by a multiplication by an orthogonal matrix. This is nicely illustrated for a planar 3R manipulator (see Fig. 1) that has a Jacobian of the form

$$J(\theta_1, \theta_2, \theta_3) = \begin{bmatrix} -a_1 s_1 - a_2 s_{12} - a_3 s_{123} & -a_2 s_{12} - a_3 s_{123} & -a_3 s_{123} \\ a_1 c_1 + a_2 c_{12} + a_3 c_{123} & a_2 c_{12} + a_3 c_{123} & a_3 c_{123} \end{bmatrix} \tag{8}$$

where the fixed a_i's are the link lengths, the variable θ_i's are the joint angles, and the remaining DH parameters have values equal to zero. (The notation s_{ijk} and c_{ijk} indicates $\sin(\theta_i + \theta_j + \theta_k)$ and $\cos(\theta_i + \theta_j + \theta_k)$, respectively.) The DH parameters are uniquely determined for a given Jacobian (8), for example, by subtracting different columns

[2]Note that our approach does not depend on our choice of fault tolerance measure. Any fault-tolerant measure, e.g., relative manipulability, can be used to define a locally optimally failure tolerant Jacobian. In fact, any local desired property defined by a Jacobian can be used in our approach.

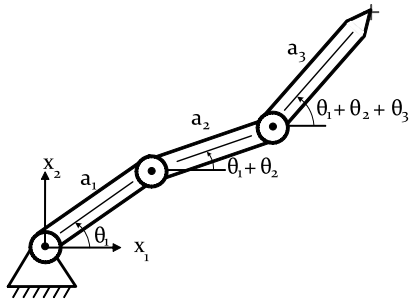

Fig. 1. A simple three degree-of-freedom planar manipulator.

to isolate specific terms in (8). If the base frame is changed by a rotation, represented here by a 2×2 rotation matrix $R(\phi)$, the manipulator's Jacobian becomes

$$J'(\theta_1, \theta_2, \theta_3) = R(\phi)J(\theta_1, \theta_2, \theta_3) = J(\theta_1 + \phi, \theta_2, \theta_3) \quad (9)$$

where $R(\phi)$ is the standard rotation matrix corresponding to a counterclockwise rotation of ϕ radians about the x_3-axis. The DH parameters of the robot corresponding to the new Jacobian $J'(\theta_1, \theta_2, \theta_3)$ are the same as they were for J with the exception that θ_1 is now replaced with $\theta_1 + \phi$. Consider now the reflection matrix $F = \mathrm{diag}(-1, 1)$, which corresponds to a reflection about the x_2–x_3 plane. Then, the modified Jacobian resulting from pre-multiplying by F is

$$J'(\theta_1, \theta_2, \theta_3) = FJ(\theta_1, \theta_2, \theta_3) = J(-\theta_1, -\theta_2, -\theta_3). \quad (10)$$

The new DH parameters are the same except that the joint angles are the negatives of the original joint angles, giving a left-handed version of the same robot. More generally, any orthogonal matrix can be written in the form $R(\phi)$ or $Q = R(\phi)F$ for a suitable angle ϕ so that pre-multiplying (1) by Q results in the Jacobian

$$QJ(\theta_1, \theta_2, \theta_3) = J(-\theta_1 + \phi, -\theta_2, -\theta_3). \quad (11)$$

Because optimal fault tolerance can be formulated in terms of the Gram matrix, it is desirable to identify the family of DH parameter sets that result in optimally fault-tolerant configurations. The unique DH parameters for a planar 3R robot are easily obtained from (8) by examining the matrix $[j_1 - j_2 \quad j_2 - j_3 \quad j_3]$, e.g., the column norms of this new matrix are equal to the corresponding a_i values. This observation generalizes for any planar n-R robot. One could also obtain the values for a_i from the Gram matrix by noting that for $i = 1, 2, \ldots, n-1$

$$\begin{aligned} a_i^2 &= \|j_i - j_{i+1}\|^2 \\ &= \|j_i\|^2 + \|j_{i+1}\|^2 - 2j_i \cdot j_{i+1} \\ &= g_{ii} + g_{i+1,i+1} - 2g_{i,i+1} \end{aligned} \quad (12)$$

and

$$a_n^2 = \|j_n\|^2 = g_{nn} \quad (13)$$

where $g_{i,i+1}$ is the $(i, i+1)$ element of G. Thus, for planar n-R manipulators, a given Gram matrix G determines a family of equivalent manipulators, each with the same set of a_i parameters determined by the square root of a simple linear combination of elements in G.

Another important question is whether one can identify other optimally fault-tolerant designs from a given Jacobian that are not equivalent by pre-multiplication by an orthogonal matrix. It is clear from the definition of optimal fault tolerance that rearranging the columns of J or multiplying one or more of the columns of J by -1 will not affect local fault tolerance; however, this will typically result in a very different manipulator. We will say that J and J' are *similar* if one is obtained from the other by permuting and/or multiplying the columns of a Jacobian by -1. In other words, J and J' are similar if $J' = JS$, where S is an $n \times n$ matrix corresponding to the desired signed permutation of the columns of J. For convenience, we will say that J and J' are *nontrivially similar* if $S \neq \pm I$. We are interested in similar Jacobians because they share the same fault tolerance properties but generally correspond to fundamentally different manipulators. The Gram matrix G' corresponding to J' is obtained from the original Gram matrix G simply by applying the same row and column operations that were used to obtain J' from J. Consequently, one can easily obtain the a_i parameters for any similar Jacobian directly from the original G for the case of planar revolute manipulators. This will be illustrated in the next section.

IV. Examples of Manipulators with Optimal Fault-Tolerant Jacobians

As mentioned earlier [40], the restrictions imposed by this definition of fault tolerance limits the number of possible robot geometries. To see this, consider the problem of identifying all planar 3R manipulators with an optimally fault-tolerant Jacobian J. When the 2×3 Jacobian J is isotropic with unit singular values, we have

$$G = J^T J = I - \hat{\mathbf{n}}_J \hat{\mathbf{n}}_J^T. \quad (14)$$

Fault tolerance requires that the components of $\hat{\mathbf{n}}_J$ have the same magnitude. However, replacing $\hat{\mathbf{n}}_J$ with $-\hat{\mathbf{n}}_J$ does not affect (2), so we only need to check the four cases $\hat{\mathbf{n}}_J = 1/\sqrt{3}\,[1 \quad \pm 1 \quad \pm 1]^T$. These four unit null vectors determine four families of nonequivalent Jacobians, each corresponding to one of the four possibilities for $I - \hat{\mathbf{n}}_J \hat{\mathbf{n}}_J^T$, which together identify all Jacobians that are optimally fault tolerant.

The optimally fault-tolerant Jacobian given in (5) corresponds to the case when the elements of $\hat{\mathbf{n}}_J$ are all positive and equal. In this case, the Gram matrix corresponding to the positional Jacobian is

$$G = \begin{bmatrix} \frac{2}{3} & -\frac{1}{3} & -\frac{1}{3} \\ -\frac{1}{3} & \frac{2}{3} & -\frac{1}{3} \\ -\frac{1}{3} & -\frac{1}{3} & \frac{2}{3} \end{bmatrix}. \quad (15)$$

The link length parameters for this particular G are then $a_1 = a_2 = \sqrt{\frac{2}{3} + \frac{2}{3} - 2(\frac{-1}{3})} = \sqrt{2}$ and $a_3 = \sqrt{2/3}$. From the family of similar Gram matrices obtained through permutations and multiplications by -1 as described earlier, one can easily deduce that the only possible link length values for an optimally fault-tolerant planar 3R manipulator are $L_l = \sqrt{2}$ and $L_s = \sqrt{2/3}$, which are obtained by using off-diagonal elements that equal $\pm\frac{1}{3}$ and diagonal elements equal to $\frac{2}{3}$. Furthermore, the square root of a diagonal value of G is equal to the distance of the end effector from the corresponding joint. In this case, each joint lies on a circle of radius $\sqrt{2/3}$ centered at the end effector with the two possible link lengths $\sqrt{2}$ and $\sqrt{2/3}$, which necessarily place the joints on the vertices of an inscribed hexagon. The four optimally fault-tolerant manipulators are described by the link lengths in Table I and illustrated in Fig. 2.

As a further example of an optimally fault-tolerant manipulator, consider a planar 4R robot. The requirements for optimal fault tolerance are that the Jacobian is isotropic and that the null space matrix N, which consists of two orthonormal null vectors of J, has the properties that its rows each have a norm of $1/\sqrt{2}$ and that the angles between

TABLE I
FOUR DIFFERENT LINK LENGTH COMBINATIONS OF (5)

Robot	a_1	a_2	a_3
1	L_s	L_s	L_s
2	L_s	L_l	L_s
3	L_l	L_s	L_s
4	L_l	L_l	L_s

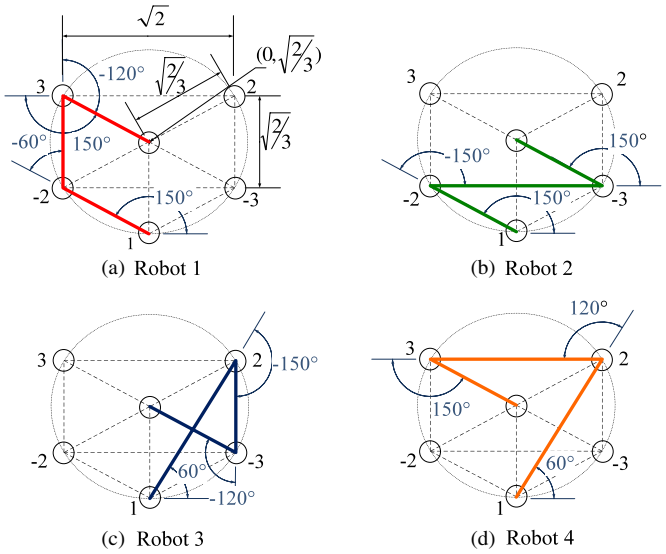

Fig. 2. A simple three degree-of-freedom planar robot that corresponds to the optimal fault-tolerant Jacobian given by (5) is shown in (d). The three other manipulators that have the same properties of the Jacobian in (5) are shown in (a)–(c).

successive rows are $45°$. Any other null space matrix related to N by a row permutation and/or the multiplication of one or more rows by -1 will also result in an optimally fault-tolerant Jacobian. The corresponding Jacobian would be given by applying the same operations to the columns of the original Jacobian. An example of a suitable Jacobian is

$$J = \begin{bmatrix} \frac{1}{\sqrt{2}} & \frac{1}{2} & 0 & -\frac{1}{2} \\ 0 & \frac{1}{2} & \frac{1}{\sqrt{2}} & \frac{1}{2} \end{bmatrix} \tag{16}$$

and its corresponding Gram matrix is

$$G = \begin{bmatrix} \frac{1}{2} & \frac{1}{2\sqrt{2}} & 0 & \frac{-1}{2\sqrt{2}} \\ \frac{1}{2\sqrt{2}} & \frac{1}{2} & \frac{1}{2\sqrt{2}} & 0 \\ 0 & \frac{1}{2\sqrt{2}} & \frac{1}{2} & \frac{1}{2\sqrt{2}} \\ \frac{-1}{2\sqrt{2}} & 0 & \frac{1}{2\sqrt{2}} & \frac{1}{2} \end{bmatrix}. \tag{17}$$

From the diagonal elements of (17), it follows that the joints of the manipulator are located on a circle of radius $1/\sqrt{2}$ centered at the end effector. The link lengths for this particular G are $a_i = \sqrt{1 - \frac{1}{\sqrt{2}}}$ for $i = 1, 2, 3$, and $a_4 = \frac{1}{\sqrt{2}}$. It will be shown below that the four potential link lengths for similar Gram matrices are $L_a = \sqrt{1 - \frac{1}{\sqrt{2}}}, L_b = \frac{1}{\sqrt{2}}, L_c = 1$, and $L_d = \sqrt{1 + \frac{1}{\sqrt{2}}}$. Consequently, it follows that the joints of an optimally fault-tolerant planar 4R manipulator appear on the vertices of an octagon inscribed on a circle of radius $\frac{1}{\sqrt{2}}$ centered at the end effector. The list of all possible manipulators is presented in Table II and depicted in Fig. 3.

TABLE II
FOURTEEN DIFFERENT LINK LENGTH COMBINATIONS OF (16)

Robot	a_1	a_2	a_3	a_4
1	L_a	L_a	L_a	L_b
2	L_a	L_c	L_a	L_b
3	L_d	L_a	L_a	L_b
4	L_a	L_a	L_d	L_b
5	L_a	L_d	L_a	L_b
6	L_c	L_a	L_c	L_b
7	L_a	L_c	L_d	L_b
8	L_d	L_c	L_a	L_b
9	L_a	L_d	L_d	L_b
10	L_d	L_d	L_a	L_b
11	L_d	L_a	L_d	L_b
12	L_c	L_d	L_c	L_b
13	L_d	L_c	L_d	L_b
14	L_d	L_d	L_d	L_b

These possible robots resulted from the fact that all possible permutations and multiplications by -1 of the columns of (16) result in the second diagonal of (17) (i.e., the diagonal above the main diagonal) being in exactly one of three forms, i.e., (x,y,z), (x,0,z), or (0,y,0), where each x, y, and z can be either $\pm\frac{1}{2\sqrt{2}}$. Thus, the total number of distinct link lengths is: $2^3 = 8$ for the (x,y,z) case plus $2^2 = 4$ for the (x,0,z) case plus $2^1 = 2$ for the (0,y,0) case resulting in 14 different manipulator designs. Note that not every manipulator with the property that it's joints are located in the vertices of this octagon are optimally fault tolerant, but the Gram matrix clearly identifies this requirement for the family of optimally fault-tolerant manipulators.

The next section discusses the global fault-tolerant behavior of both the 3R and 4R families of manipulators, and shows how the robots within the same family are still quite different as they act differently beyond the design point.

V. ANALYSIS AND COMPARISON OF MANIPULATOR DESIGNS

The fact that there are multiple manipulator designs with the same desired local fault tolerance properties allows one to use other criteria to select a preferred design. In particular, while the robots all share the same local properties at the given configuration, they are quite different in terms of their global properties. For example, first consider the 3R robots defined in Table I and Fig. 2. Even when joint limits are not considered, their workspaces are quite different, e.g., the maximum reach will be either $3L_s, 2L_s + L_l$, or $L_s + 2L_l$. More importantly, if one is concerned with fault-tolerance, the values of the proposed fault-tolerance measure vary significantly for these four robot designs.

To determine how the fault tolerance measure $\mathcal{K}$ varies as a robot moves away from the configuration that has the optimal Jacobian, the optimal value of $\mathcal{K}$ was computed for every location within each of the four robot's workspaces. Because $\mathcal{K}$ is not a function of θ_1, it is sufficient to compute its maximum value as a function of distance from the base of the manipulator. The maximum value of $\mathcal{K}$ is determined by computing $\mathcal{K}$ for the Jacobians of all possible robot configurations at each distance. The results of this calculation are shown in Fig. 4 for all four robots.

The first interesting point to note is that Robot 4 in Fig. 4, which is generated from the original Jacobian in (5), actually has a configuration with a larger value of $\mathcal{K}$ at the design point that is a distance of $\sqrt{2/3}$ from the base than that of the optimal value of $\mathcal{K} = \sqrt{1/3}$. This is possible because at this configuration, the Jacobian is no longer isotropic, however, its non-isotropy is due to a larger

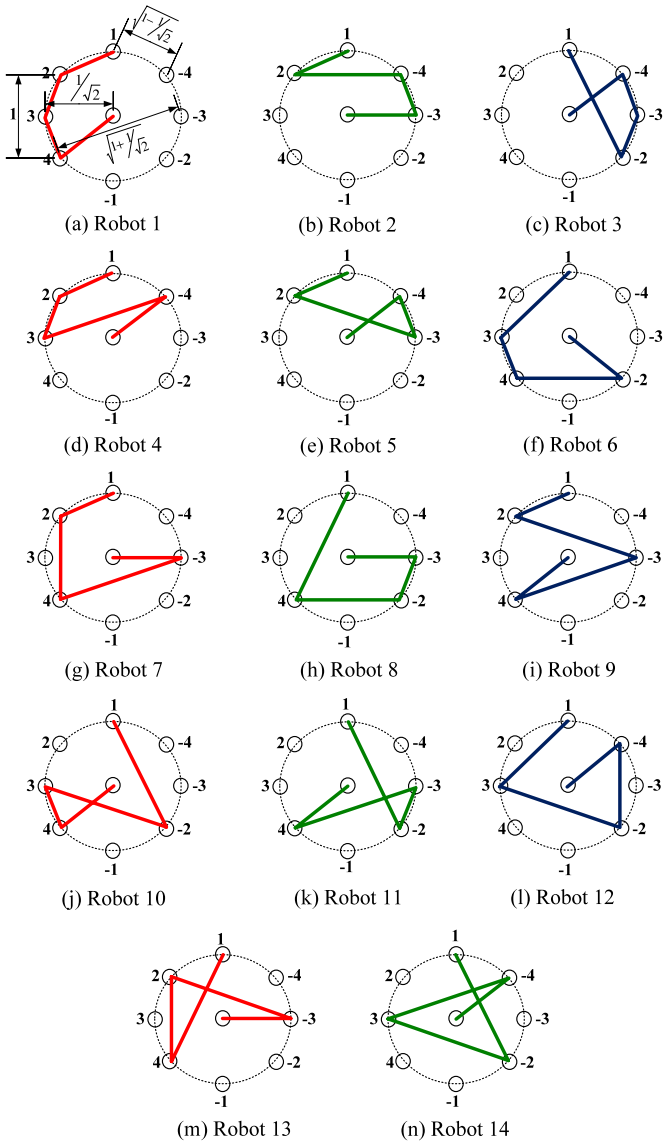

Fig. 3. A simple four degree-of-freedom planar robot that corresponds to the optimal fault-tolerant Jacobian given by (16) is shown in (a). The other 13 manipulators that have the same properties of the Jacobian in (16) are shown in (b) to (n).

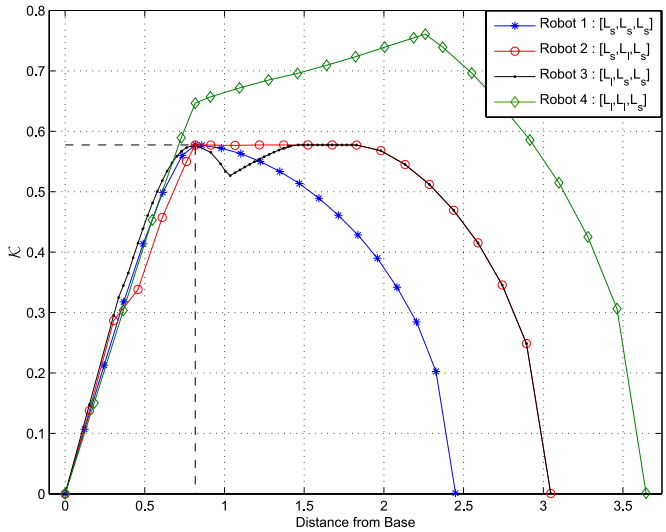

Fig. 4. The relationship between the maximum value of $\mathcal{K}$ and the distance from the base for Robots 1, 2, 3, and 4 in Table I.

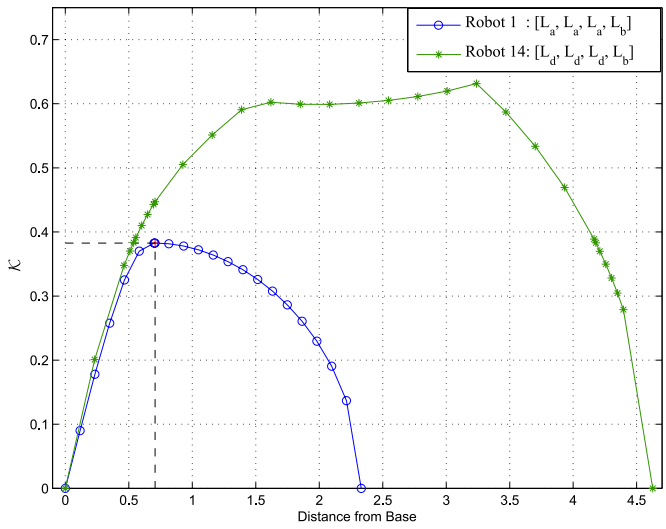

Fig. 5. The relationship between $\mathcal{K}$ and the distance from the base for Robots 1 and 14 in Table II.

maximum singular value, and may not be considered undesirable. In addition, the value of $\mathcal{K}$ is significantly higher than the optimal value for a significant portion of this manipulator's workspace, making it particularly well suited for applications that require failure tolerance.

In contrast, consider Robot 1 in Fig. 4. It has a value of $\mathcal{K} = \sqrt{1/3}$ at the optimal distance as designed, however, this is its peak value of $\mathcal{K}$, and $\mathcal{K}$ is monotonically decreasing away from this point. Thus, in addition to having the smallest workspace, this manipulator has a significantly smaller tolerance to joint failures throughout its workspace.

The characteristics of the two medium length robots, i.e., Robots 2 and 3 in Fig. 4, fall somewhat in between the two extremes just described, but exhibit important differences. Robot 2 has a flat region for the maximum value of $\mathcal{K}$ in the middle of its workspace. (See the Appendix for a proof of why $\mathcal{K}$ is constant in this region.) In contrast, Robot 3 has a significant dip in the maximum value of $\mathcal{K}$ at a distance near one unit from the base before it returns to a comparable value to that of Robot 2.

Similarly, the fourteen robots in Table II have different workspace properties, e.g., Robot 1 has the smallest maximum reach of $3L_a + L_b$ and Robot 14 has the largest at $3L_d + L_b$. Fig. 5 illustrates how Robots 1 and 14 are also different in terms of the fault tolerance measure with respect to the distance from the base for the case of two joint failures. Robot 1 has a peak in $\mathcal{K}$ at its optimal value of $\frac{1}{2}\sqrt{1-\frac{1}{\sqrt{2}}}$ at the design point, with $\mathcal{K}$ decreasing relatively rapidly away from this point. In contrast, Robot 14 has a larger value of $\mathcal{K}$ at the design point than the optimal value of $\mathcal{K}$ which is because of the fact that at this configuration the Jacobian is no longer isotropic. Moreover, the value of $\mathcal{K}$ is significantly higher than the optimal value for a large portion of this manipulator's workspace.

Table III presents a comparison of the different global properties for the 14 robots shown in Fig. 3. The fault-tolerant workspace percentage column is a measure of the ratio of fault-tolerant workspace, in which $\mathcal{K}$ is greater than or equal to the value at the design point, to the total workspace. The average amount of joint motion per meter needed to stay at the configuration with the maximum value of $\mathcal{K}$ throughout the

TABLE III
FAULT-TOLERANT WORKSPACE ANALYSIS OF THE FOURTEEN ROBOTS IN TABLE II

Robot	Reach $[m]$	Fault tolerant workspace [%]	Joint motion $[^\circ/m]$
1	2.33	0.00	–
2	2.79	15.14/(0.25)	107.3
3	3.10	9.99/(0.07)	117.0
4	3.10	22.16/(1.31)	98.6
5	3.10	26.96/(0.73)	372.8[1]
6	3.25	47.76	94.1
7	3.56	46.21/(0.04)	190.2[2]
8	3.56	49.06/(0.10)	72.2
9	3.86	57.68	79.7
10	3.86	58.02	109.8
11	3.86	58.78	71.0
12	4.01	73.03	76.5
13	4.32	77.42	74.1
14	4.63	80.23	70.7

[1] Robot 5 has two algorithmic singularities. Choosing the fault-tolerant workspace bound before the first algorithmic singularity point gives us the fault-tolerant workspace percentage of 6.3%, and joint motion of 84.1 °/m.
[2] Robot 7 has one algorithmic singularity. Similar to Robot 5, if we choose the fault-tolerant workspace bound of Robot 7 before the algorithmic singularity point, the fault-tolerant workspace percentage is 30.8%, and joints motion is 70.8 °/m.

fault-tolerant workspace is shown in the last column. Note that Robots 5 and 7 have much larger values for this measure because these robots encounter algorithmic singularities within the workspace that require a significant amount of reconfiguration for the robot to stay at the maximum value of $\mathcal{K}$. Robots 2, 3, 4, 5, 7, and 8 have the fault-tolerant workspace separated into two pieces, i.e., there is a region in between where the maximum of $\mathcal{K}$ drops below the optimal value. (Similar is to that of Robot 3 in the 3R case shown in Fig. 2.) The amount of this drop varies depending upon the robot, ranging from as small as 0.2% for Robots 4 and 8, to as large as 9% for Robot 3. The number between parentheses is the smaller of the two fault-tolerant workspaces, which in all cases includes the design point.

Clearly, the maximum reach (or sum of the link lengths) has a dominant effect on the global fault-tolerant properties.[3] However, there are three cases where the same maximum reach can be obtained by multiple different robot designs with significant differences in their global fault-tolerant properties. Consider first the case of Robots 9–11. Even though their fault-tolerant workspace percentages are almost the same, there is a significant difference in the amount of joint motion needed to maintain a fault-tolerant configuration. In particular, Robot 11 only moves a total of 177 degrees to traverse the entire fault-tolerant region, whereas Robots 9 and 10 take 191 and 263 degrees, respectively, to do so. This is visually illustrated in Fig. 6 where for each robot three different optimal configurations are shown. (The blue one is at the design point, the green one is at a boundary of the fault-tolerant workspace, and the red configuration is at the middle.) Furthermore, the joint motion is distributed differently for the three robots, with Robot 9 requiring much less motion in joint one, which may be desirable due to the large moment of inertia associated with this joint.

[3] It is important to note that one can always scale these robot designs to obtain any desired maximum reach, which is why we normalize the fault-tolerant workspace results in Table III to be a percentage.

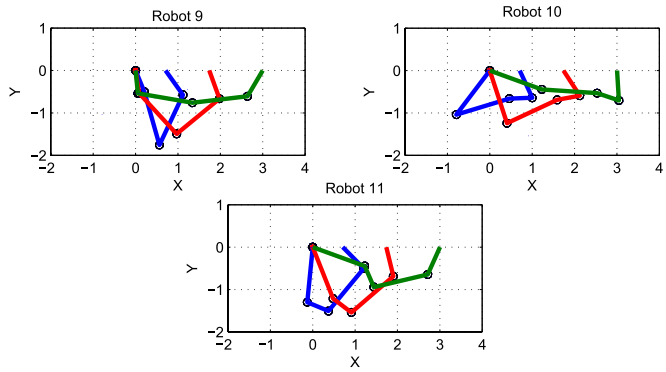

Fig. 6. Three different configurations with maximum $\mathcal{K}$ at three different points along the x-axis trajectory for Robots 9–11. In all cases, the first configuration is from the design point at a distance of $1/\sqrt{2}$, and the last configuration is at the boundary of the fault-tolerant workspace at a distance of approximately three.

Robots 3–5 also represent a group with equal reach but different global properties. If one only considers percentage of fault-tolerant workspace, then Robot 3 is the worst (at 10%), and Robot 5 is the best (at 27%). However, Robot 5 encounters two algorithmic singularities within this region, which require the robot to reconfigure itself to a new posture in order to maintain $\mathcal{K}$ at its maximum value. This results in excessive joint motion over a very short period of time. If one opts to avoid this reconfiguration and follows the locally optimal value of $\mathcal{K}$, then $\mathcal{K}$ will monotonically decrease and results in a fault-tolerant workspace percentage of only 6.3%. This is illustrated in Fig. 7. Thus, one could argue that Robot 4 is the best design out of the three.

VI. EIGHT DEGREE-OF-FREEDOM MANIPULATOR EXAMPLE

In this section, we present the design of a locally optimal eight degree-of-freedom manipulator operating in a fully six-dimensional task space in order to illustrate the generality of our approach. An example of an optimally failure tolerant Jacobian for such a manipulator is given by (18) at the bottom of the page. This Jacobian satisfies the optimality equation (4) and is isotropic with equal singular values of

$$\sigma = \sqrt{n/3} = \sqrt{8/3} \tag{19}$$

$$J = \begin{bmatrix} 0 & 0.6865 & -0.1131 & 0.2439 & 0.9231 & -0.3824 & -0.8152 & -0.6783 \\ 1 & -0.7116 & 0.3662 & 0.4505 & -0.3829 & -0.4760 & -0.1903 & -0.6432 \\ 0 & 0.1497 & -0.9236 & 0.8588 & -0.0354 & -0.7919 & 0.5469 & 0.3553 \\ 0 & 0.6475 & 0.4213 & 0.9106 & -0.1928 & 0.8022 & 0.5691 & -0.4861 \\ 0 & 0.6919 & 0.8595 & 0.1982 & -0.5402 & -0.5963 & -0.4379 & 0.7554 \\ 1 & 0.3197 & 0.2893 & -0.3626 & 0.8190 & -0.0289 & 0.6960 & 0.4396 \end{bmatrix}. \tag{18}$$

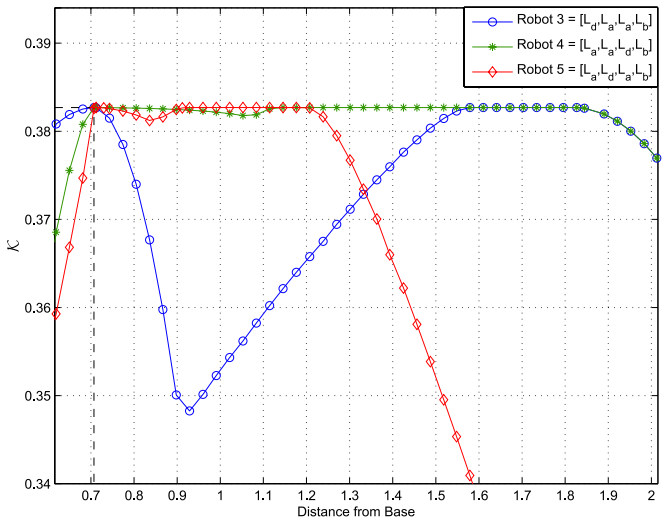

Fig. 7. The relationship between $\mathcal{K}$ and the distance from the base for Robots 3–5. The plot focuses on the behavior near the design point to highlight the difference in this region. Note that the value of $\mathcal{K}$ for Robot 5 is shown for joint motion that does not include a discontinuity due to an algorithmic singularity. If the discontinuous joint motion is performed, then the $\mathcal{K}$ value for Robot 5 is comparable to that of Robot 4.

TABLE IV
DH PARAMETERS OF THE ROBOT WHOSE JACOBIAN IS GIVEN BY (18)

i	$\alpha_i\,[^\circ]$	$a_i\,[m]$	$\theta_i\,[^\circ]$	$d_i\,[m]$
1	71	−0.89	137	0
2	16	1.41	86	−2.52
3	63	−1.17	−136	2.35
4	125	−1.46	−86	1.09
5	82	−0.66	151	−1.83
6	46	1.56	147	0.61
7	108	−0.67	−20	1.56
8	0	1	−81	1.21

and an optimal worst-case failure tolerance of

$$^f\sigma_6 = \sqrt{8/3}\cdot\sqrt{2/8} = \sqrt{2/3}. \tag{20}$$

The DH parameters of this robot are given in Table IV. One way of realizing this robot at the design point is shown in Fig. 8. If one performs a global analysis as described above, the end-effector can be moved away from the design point a distance of 2.3 m and maintain a $\mathcal{K}$ value that is 90% of the optimal. This configuration is illustrated in Fig. 9.

As is in the planar case, one can perform various operations on this manipulator Jacobian to obtain different corresponding robots that still have the property of optimal fault tolerance at the design point. Consequently, the designer has a significant amount of freedom in choosing the robot geometry. For example, permuting the columns of (18) would result in an optimally fault-tolerant Jacobian that corresponds to a different manipulator. However, portions of the DH table corresponding to the modified Jacobian may reappear from the original DH table when three or more successive columns of the original Jacobian appear in that order. In this case, the manipulators will share some similarities in geometry. Unlike the planar case, multiplying a column of the Jacobian by -1 only changes the direction of the corresponding axis of rotation and does not essentially change the robot geometry.

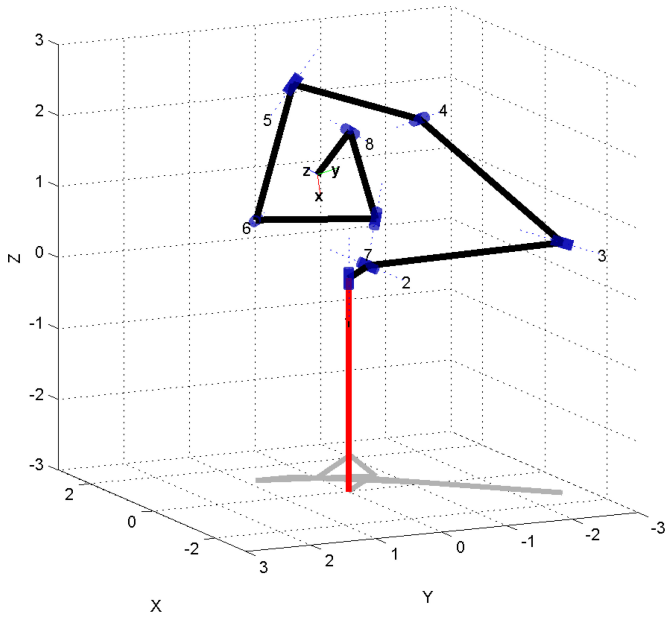

Fig. 8. The eight degree-of-freedom robot that is given in Table IV. This configuration corresponds to the design point for the optimal failure tolerant Jacobian given in (18).[4]

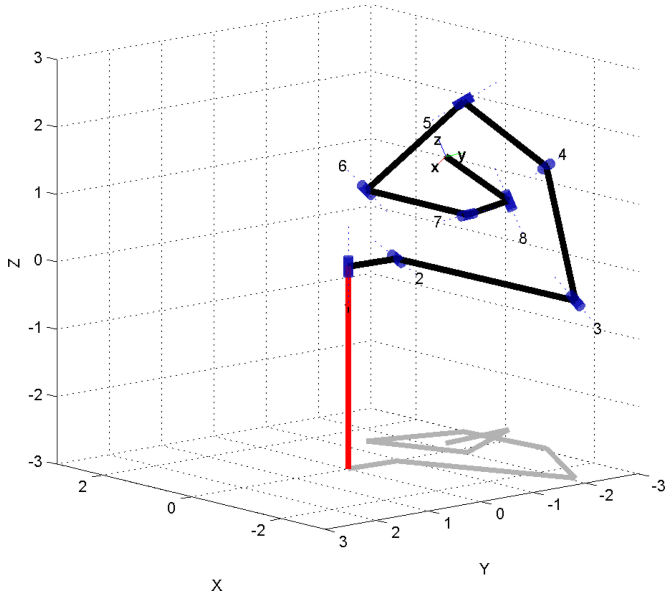

Fig. 9. The configuration of the eight degree-of-freedom robot that has $\mathcal{K}$ at 90% of the optimal $\mathcal{K}$ value, which occurs with the end-effector position 2.3 m away from the design point.[4]

VII. CONCLUSION

It has been previously shown that there are multiple different robot designs that possess the same desired Jacobian at a specific operating point. This work has presented a mathematical analysis, based on the Gram matrix, that allows one to enumerate all of the possible planar manipulators that possess certain desired fault tolerance properties based on the form of a desired Jacobian. This analysis was illustrated on both a 3R manipulator experiencing a single locked joint failure and a 4R manipulator experiencing two joint failures. It was further shown

[4] This graphic was generated using the Robotics Toolbox described in [46].

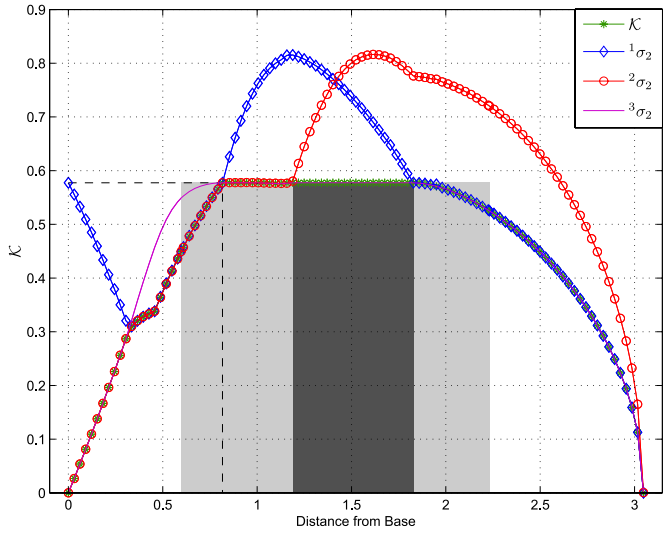

Fig. 10. The relationship between $\mathcal{K}$ and the distance from the base for Robot 2 in Table I. The minimum singular values for all possible failures are shown for the configuration that maximizes $\mathcal{K}$. Note that if only $\mathcal{K}_3$ were being optimized, then it would be constant for a larger range.

that there are significant differences in the capabilities of the resulting manipulators, both in terms of pre- and pos-tfailure performance. It was shown that some of these differences are related to the fact that the same Jacobian can result in manipulators that vary significantly in workspace area. However, it is quite surprising that major differences in behavior were also found in manipulator designs that were identical in terms of area.

APPENDIX

EXPLANATION OF WHY $\mathcal{K}$ IS CONSTANT FOR ROBOT 2 IN FIG. 4

A striking feature of Fig. 4 is the flat region of the plot of $\mathcal{K}$ for Robot 2. In this Appendix, it will be shown that the maximum value of $^3\sigma_2$ for Robot 2 is actually constant for a range of distances from the base that includes the flat region in Fig. 4. In the case of the analysis for Robot 2 in Fig. 4, the critical failure happens to be joint 3 over the region where $\mathcal{K}$ is flat (see Fig. 10).

We begin by noting that the singular values of the reduced Jacobian

$$^3J = \begin{bmatrix} -a_1 s_1 - a_2 s_{12} - a_3 s_{123} & -a_2 s_{12} - a_3 s_{123} \\ a_1 c_1 + a_2 c_{12} + a_3 c_{123} & a_2 c_{12} + a_3 c_{123} \end{bmatrix} \tag{A1}$$

are equal to the square roots of the eigenvalues of

$$(^3J)^T(^3J) = \begin{bmatrix} \|j_1\|^2 & j_1 \cdot j_2 \\ j_1 \cdot j_2 & \|j_2\|^2 \end{bmatrix} \tag{A2}$$

which are readily given by the characteristic equation of (A2). In particular, the minimum singular value $^3\sigma_2$ of (A1) is given by the relationship

$$2(^3\sigma_2)^2 = \|j_1\|^2 + \|j_2\|^2 - \sqrt{(\|j_1\|^2 - \|j_2\|^2)^2 + 4(j_1 \cdot j_2)^2}. \tag{A3}$$

From (A1), one has that $\|j_1\|$ is equal to the distance d from the base to the end effector and that $\|j_1 - j_2\|$ is equal to the first link length a_1, which together imply that

$$j_1 \cdot j_2 = \frac{1}{2}[\|j_1\|^2 + \|j_2\|^2 - \|j_1 - j_2\|^2] = \frac{1}{2}[d^2 + \|j_2\|^2 - a_1^2]. \tag{A4}$$

The expression for (A3) can then be written as

$$2(^3\sigma_2)^2 = z + d^2 - \sqrt{(z - d^2)^2 + (z + d^2 - a_1^2)^2} \tag{A5}$$

where, for convenience, we have introduced the notation $z = \|j_2\|^2$. Since the link length a_1 is fixed, we have that, for a specified end-effector distance d, (A5) is a function of the single variable z, which we shall denote by $g(z)$.

Setting the derivative of

$$g(z) = z + d^2 - \sqrt{(z - d^2)^2 + (z + d^2 - a_1^2)^2} \tag{A6}$$

to zero, one obtains a single extremal point whose value depends on whether d is greater than, less than, or equal to $a_1/\sqrt{2}$. This extremal point can be conveniently written as $z^* = \max(d^2, a_1^2 - d^2)$. The case of interest here is when $d > a_1/\sqrt{2}$. In this case, we have that $z^* = d^2$, $g'(z^*) = 0$, and $g''(z) < 0$ for all z. It then follows that $z^* = d^2$ results in a maximum value of $g(z^*) = a_1^2$, regardless of the specific value of d. For the robot to achieve $z = \|j_2\|^2 = d^2$, it is necessary and sufficient that $|a_2 - a_3| \le d \le a_2 + a_3$ due to the geometric constraints on $\|j_2\|$ associated with the lengths of the second and third links. In summary, if $d > a_1/\sqrt{2}$ and $|a_2 - a_3| \le d \le a_2 + a_3$, then the value of $\mathcal{K}_3(d)$ is equal to $a_1/\sqrt{2}$, where $\mathcal{K}_3(d)$ denotes the maximum value of $^3\sigma_2$ over all configurations where the end effector is at a distance d from the base. It is interesting to note that this solution corresponds to the end effector being equally distant from the base and the second joint. Depending on the values of d and the link lengths a_i, these conditions may or may not be possible due to the geometry of the robot. In the case of Robot 2, $a_1/\sqrt{2} = 1/\sqrt{3} = 0.5774$, $|a_2 - a_3| = 0.5977$, and $a_2 + a_3 = 2.2307$, and we conclude that $\mathcal{K}_3 = 0.5774$ over the range $0.5977 \le d \le 2.2307$.

REFERENCES

[1] K. N. Groom, A. A. Maciejewski, and V. Balakrishnan, "Real-time failure-tolerant control of kinematically redundant manipulators," *IEEE Trans. Robot. Autom.*, vol. 15, no. 6, pp. 1109–1116, Dec. 1999.

[2] Reliability Information Analysis Center, "Nonelectronic parts reliability data," *Defense Tech. Inform. Center/Air Force Res. Lab*, Rome, NY, USA, no. NPRD-2011, 2011.

[3] B. S. Dhillon A. R. M. Fashandi and K. L. Liu, "Robot systems reliability and safety: A review," *J. Quality Maintenance Eng.*, vol. 8, no. 3, pp. 170–212, 2002.

[4] H. Nakata, "Domestic robots failed to ride to rescue after No. 1 plant blew," *Japan Times*, Jan. 6, 2012.

[5] E. C. Wu, J. C. Hwang, and J. T. Chladek, "Fault-tolerant joint development for the space shuttle remote manipulator system: Analysis and experiment," *IEEE Trans. Robot. Autom.*, vol. 9, no. 5, pp. 675–684, Oct. 1993.

[6] G. Visentin and F. Didot, "Testing space robotics on the Japanese ETS-VII satellite," *ESA Bulletin-Eur. Space Agency*, vol. 99, pp. 61–65, Sep. 1999.

[7] P. S. Babcock and J. J. Zinchuk, "Fault-tolerant design optimization: Application to an autonomous underwater vehicle navigation system," in *Proc. Symp. Auton. Underwater Vehicle Technol.*, Washington, D.C., USA, Jun. 5–6, 1990, pp. 34–43.

[8] R. Colbaugh and M. Jamshidi, "Robot manipulator control for hazardous waste-handling applications," *J. Robot. Syst.*, vol. 9, no. 2, pp. 215–250, 1992.

[9] W. H. McCulloch, "Safety analysis requirements for robotic systems in DOE nuclear facilities," in *Proc. 2nd Specialty Conf. Robot. Challenging Environ.*, Albuquerque, NM, USA, Jun. 1–6, 1996, pp. 235–240.

[10] D. L. Schneider, D. Tesar, and J. W. Barnes, "Development & testing of a reliability performance index for modular robotic systems," in *Proc. Annu. Rel. Maintain. Symp.*, Anaheim, CA, USA, Jan. 24–27, 1994, pp. 263–271.

[11] C. J. J. Paredis and P. K. Khosla, "Designing fault-tolerant manipulators: How many degrees of freedom?," *Int. J. Robot. Res.*, vol. 15, no. 6, pp. 611–628, Dec. 1996.

[12] S. Tosunoglu and V. Monteverde, "Kinematic and structural design assessment of fault-tolerant manipulators," *Intell. Autom. Soft Comput.*, vol. 4, no. 3, pp. 261–268, 1998.

[13] C. Carreras and I. D. Walker, "Interval methods for fault-tree analysis in robotics," *IEEE Trans. Robot. Autom.*, vol. 50, no. 1, pp. 3–11, Mar. 2001.
[14] M. L. Visinsky, J. R. Cavallaro, and I. D. Walker, "A dynamic fault tolerance framework for remote robots," *IEEE Trans. Robot. Autom.*, vol. 11, no. 4, pp. 477–490, Aug. 1995.
[15] L. Notash, "Joint sensor fault detection for fault tolerant parallel manipulators," *J. Robot. Syst.*, vol. 17, no. 3, pp. 149–157, 2000.
[16] M. Leuschen, I. Walker, and J. Cavallaro, "Fault residual generation via nonlinear analytical redundancy," *IEEE Trans. Control Syst. Tech.*, vol. 13, no. 3, pp. 452–458, May 2005.
[17] M. Anand, T. Selvaraj, S. Kumanan, and J. Janarthanan, "A hybrid fuzzy logic artificial neural network algorithm-based fault detection and isolation for industrial robot manipulators," *Int. J. Manuf. Res.*, vol. 2, no. 3, pp. 279–302, 2007.
[18] D. Brambilla, L. Capisani, A. Ferrara, and P. Pisu, "Fault detection for robot manipulators via second-order sliding modes," *IEEE Trans. Ind. Electron.*, vol. 55, no. 11, pp. 3954–3963, Nov. 2008.
[19] J. Park, W.-K. Chung, and Y. Youm, "Failure recovery by exploiting kinematic redundancy," in *Proc. 5th Int. Workshop Robot Human Commun.*, Tsukuba, Japan, Nov. 11–14, 1996, pp. 298–305.
[20] X. Chen and S. Nof, "Error detection and prediction algorithms: Application in robotics," *J. Intell. Robot. Syst.; Robot. Syst.*, vol. 48, no. 2, pp. 225–252, 2007.
[21] M. Ji and N. Sarkar, "Supervisory fault adaptive control of a mobile robot and its application in sensor-fault accommodation," *IEEE Trans. Robot.*, vol. 23, no. 1, pp. 174–178, Feb. 2007.
[22] A. De Luca and L. Ferrajoli, "A modified NewtonEuler method for dynamic computations in robot fault detection and control," in *Proc. IEEE Int. Conf. Robot. Autom.*, May 2009, pp. 3359–3364.
[23] Y. Ting, S. Tosunoglu, and B. Fernandez, "Control algorithms for fault-tolerant robots," in *Proc. IEEE Int. Conf. Robot. Autom.*, May 8–13, 1994, vol. 2, pp. 910–915.
[24] J. D. English and A. A. Maciejewski, "Fault tolerance for kinematically redundant manipulators: Anticipating free-swinging joint failures," *IEEE Trans. Robot. Autom.*, vol. 14, no. 4, pp. 566–575, Aug. 1998.
[25] J. D. English and A. A. Maciejewski, "Failure tolerance through active braking: A kinematic approach," *Int. J. Robot. Res.*, vol. 20, no. 4, pp. 287–299, Apr. 2001.
[26] P. Nieminen, S. Esque, A. Muhammad, J. Mattila, J. Väyrynen, M. Siuko, and M. Vilenius, "Water hydraulic manipulator for fail safe and fault tolerant remote handling operations at ITER," *Fusion Eng. Design*, vol. 84, no. 7, pp. 1420–1424, 2009.
[27] J. E. McInroy, J. F. O'Brien, and G. W. Neat, "Precise, fault-tolerant pointing using a Stewart platform," *IEEE/ASME Trans. Mechatronics*, vol. 4, no. 1, pp. 91–95, Mar. 1999.
[28] M. Hassan and L. Notash, "Optimizing fault tolerance to joint jam in the design of parallel robot manipulators," *Mech. Mach. Theory*, vol. 42, no. 10, pp. 1401–1417, 2007.
[29] Y. Chen, J. E. McInroy, and Y. Yi, "Optimal, fault-tolerant mappings to achieve secondary goals without compromising primary performance," *IEEE Trans. Robot.*, vol. 19, no. 4, pp. 680–691, Aug. 2003.
[30] Y. Yi, J. E. McInroy, and Y. Chen, "Fault tolerance of parallel manipulators using task space and kinematic redundancy," *IEEE Trans. Robot.*, vol. 22, no. 5, pp. 1017–1021, Oct. 2006.
[31] J. E. McInroy and F. Jafari, "Finding symmetric orthogonal Gough–Stewart platforms," *IEEE Trans. Robot.*, vol. 22, no. 5, pp. 880–889, Oct. 2006.
[32] C. L. Lewis and A. A. Maciejewski, "Dexterity optimization of kinematically redundant manipulators in the presence of failures," *Comput. Electr. Eng.: Int. J.*, vol. 20, no. 3, pp. 273–288, May 1994.
[33] A. A. Maciejewski, "Fault tolerant properties of kinematically redundant manipulators," in *Proc. IEEE Int. Conf. Robot. Autom.*, Cincinnati, OH, USA, May 13–18, 1990, pp. 638–642.
[34] R. G. Roberts and A. A. Maciejewski, "A local measure of fault tolerance for kinematically redundant manipulators," *IEEE Trans. Robot. Autom.*, vol. 12, no. 4, pp. 543–552, Aug. 1996.
[35] R. G. Roberts, "On the local fault tolerance of a kinematically redundant manipulator," *J. Robot. Syst.*, vol. 13, no. 10, pp. 649–661, Oct. 1996.
[36] C. J. J. Paredis and P. K. Khosla, "Fault tolerant task execution through global trajectory planning," *Rel. Eng. Syst. Safety*, vol. 53, pp. 225–235, 1996.
[37] C. L. Lewis and A. A. Maciejewski, "Fault tolerant operation of kinematically redundant manipulators for locked joint failures," *IEEE Trans. Robot. Autom.*, vol. 13, no. 4, pp. 622–629, Aug. 1997.
[38] R. S. Jamisola, Jr., A. A. Maciejewski, and R. G. Roberts, "Failure-tolerant path planning for kinematically redundant manipulators anticipating locked-joint failures," *IEEE Trans. Robot.*, vol. 22, no. 4, pp. 603–612, Aug. 2006.
[39] R. G. Roberts, R. J. Jamisola, Jr., and A. A. Maciejewski, "Identifying the failure-tolerant workspace boundaries of a kinematically redundant manipulator," in *Proc. IEEE Int. Conf. Robot. Automat.*, Rome, Italy, Apr. 10–14, 2007, pp. 4517–4523.
[40] K. M. Ben-Gharbia, R. G. Roberts, and A. A. Maciejewski, "Examples of planar robot kinematic designs from optimally fault-tolerant Jacobians," in *Proc. IEEE Int. Conf. Robot. Autom.*, Shanghai, China, May 9–13, 2011, pp. 4710–4715.
[41] T. Yoshikawa, "Manipulability of robotic mechanisms," *Int. J. Robot. Res.*, vol. 4, no. 2, pp. 3–9, 1985.
[42] C. A. Klein and B. E. Blaho, "Dexterity measures for the design and control of kinematically redundant manipulators," *Int. J. Robot. Res.*, vol. 6, no. 2, pp. 72–83, 1987.
[43] C. Klein and T. A. Miklos, "Spatial robotic isotropy," *Int. J. Robot. Res.*, vol. 10, no. 4, pp. 426–437, 1991.
[44] K. E. Zanganeh and J. Angeles, "Kinematic isotropy and the optimum design of parallel manipulators," *Int. J. Robot. Res.*, vol. 16, no. 2, pp. 185–197, Apr. 1997.
[45] A. A. Maciejewski and R. G. Roberts, "On the existence of an optimally failure tolerant 7R manipulator Jacobian," *Appl. Math. Comput. Sci.*, vol. 5, no. 2, pp. 343–357, 1995.
[46] P. I. Corke, "A robotics toolbox for MATLAB," *IEEE Robot. Autom. Mag.*, vol. 3, no. 1, pp. 2–32, Mar. 1996.

Gossip-Based Centroid and Common Reference Frame Estimation in Multiagent Systems

Mauro Franceschelli and Andrea Gasparri

***Abstract*—In this study, the decentralized common reference frame estimation problem for multiagent systems in the absence of any common coordinate system is investigated. Each agent is deployed in a 2-D space and can only measure the relative distance of neighboring agents and the angle of their line of sight in its local reference frame; no relative attitude measurement is available. Only asynchronous and random pairwise communications are allowed between neighboring agents. The convergence properties of the proposed algorithm are characterized, and its sensitiveness against additive noise on the relative distance measurements is investigated. An experimental validation of the effectiveness of the proposed algorithm is provided.**

***Index Terms*—Consensus, distributed randomized algorithms, gossip, multiagent systems, sensor network localization.**

Manuscript received March 23, 2013; revised July 18, 2013; accepted November 12, 2013. Date of publication December 13, 2013; date of current version April 1, 2014. This paper was recommended for publication by Associate Editor C. C. Cheah and Editor D. Fox upon evaluation of the reviewers' comments. This work was supported in part by the funding from the European Union Seventh Framework Programme [FP7/2007-2013] under Grant agreement 257462 HYCON2 Network of excellence and in part by the Italian Grant FIRB "Futuro in Ricerca," project NECTAR "Networked Collaborative Team of Autonomous Robots," code RBFR08QWUV, funded by the Italian Ministry of Research and Education.

M. Franceschelli is with the Department of Electrical and Electronic Engineering, University of Cagliari, 09123 Cagliari, Italy (e-mail: mauro.franceschelli@diee.unica.it).

A. Gasparri is with the Department of Engineering, Roma Tre University, Rome 00146, Italy (e-mail: gasparri@dia.uniroma3.it).

Color versions of one or more of the figures in this paper are available online at http://ieeexplore.ieee.org.

Digital Object Identifier 10.1109/TRO.2013.2291621